Tomi Räsänen* and Veli-Pekka Pyrhönen

State feedback control of a rotary inverted pendulum

Abstract: In this paper, we design a state feedback controller for a rotary inverted pendulum, which is mounted to a Quanser QUBE-Servo 2 unit. To be more specific, we use linear quadratic regulator to find suitable controller gains for QUBE-Servo 2 system. The essential characteristics of the QUBE-Servo 2 unit are presented and the performances of the closed-loop systems are evaluated based on rise time, settling time and overshoot of the rotary arm's step response. The design is validated using simulations and real-time experiments. The resulting controller stabilizes the rotary pendulum to upright position and is able to move the pendulum to desired angular position while keeping the balance under control.

Keywords: LQR-control, pole-placement, inverted pendulum, balance control, reference tracking

*Corresponding Author: Tomi Räsänen: Tampere University (Bachelor's student), E-mail: tomi.rasanen@tuni.fi
Veli-Pekka Pyrhönen: Tampere University, E-mail: veli-pekka.pyrhonen@tuni.fi

1 Introduction

Regulating a link to its upright position is an application of a mechanical balancing problem. Combined with a reference tracking, it becomes an exciting problem for testing various control designs. State feedback is a widely used method for designing feedback controllers for linear-time-invariant (LTI) systems. LTI-design methods take advantage of the well-known theory of linear algebra to form simple controllers. A classical method is pole placement which, in theory, results in closed-loop system with arbitrary dynamics [1]. In practice, there are always e.g. physical restrictions that limit the achievable performance of the closed-loop control system such as parasitic effects and actuator saturation. Optimization can also be used in line with LTI-design algorithms to yield an optimal solution to the problem with given parameters. A well-known optimal control method is the linear quadratic regulator (LQR) which is one of the most important results in modern control theory [2].

Inverted pendulum systems have been studied extensively in recent years. For example, stabilization of a real inverted pendulum was studied in [3], controlling a wheeled inverted pendulum in [4] and characteristics of the control of a flying inverted pendulum in [5]. Related topics to the inverted pendulums were also studied in [6]–[8]. In this paper, we design state feedback controllers for a rotary inverted pendulum using the pole-placement and LQR design methods. The rotary inverted pendulum is attached to a Quanser QUBE-Servo 2 unit, which is a small-scale design platform for a variety of control methods. The characteristics of the system is captured by single-input–multiple-output (SIMO) model. The feedback controllers are designed to regulate the pendulum link to the upright position with carefully coordinated movements of the DC motor. Feedback control also enables the rotary arm to turn from one angle to another. The performance of the designed controllers are evaluated using the well-known classical measures such as rise time, settling time and overshoot.

The material of this paper is organized in the following order. Section 2 presents the pole-placement method and LQR-control, whereas Section 3 examines the Smith-McMillan form of the system. In Section 4, we introduce characteristics of the QUBE-Servo 2 unit and the model of the inverted pendulum. In Section 5, feedback controllers are designed and the resulting closed-loop control systems are tested using simulations as well as real-time experiments with QUBE-Servo 2 system. Finally, some concluding remarks are summarized into Section 6.

2 State feedback

In this section, a short introduction to state-space representation and state feedback law are discussed. In addition, theory of the pole-placement method and LQR-control are presented.

2.1 State-space representation

The system considered in this paper is SIMO of the following form

$$\begin{cases} \dot{\mathbf{x}}(t) & = A\mathbf{x}(t) + \mathbf{b}u(t) \\ \mathbf{y}(t) & = C\mathbf{x}(t), \end{cases} \quad \mathbf{x}(t_0) = \mathbf{x}_0 \quad (1)$$

where $A \in \mathbb{R}^{n \times n}$ is the system matrix, $\mathbf{x} \in \mathbb{R}^n$ is the state vector, $u \in \mathbb{R}$ is control input, and vector $\mathbf{b} \in \mathbb{R}^{n \times 1}$. Output matrix $C \in \mathbb{R}^{1 \times n}$ describes the relationship between state vector and output vector $\mathbf{y} \in \mathbb{R}^{1 \times 1}$, which includes the angle measurements from the system. The system (1) is said to be realization $(A, \mathbf{b}, C)$.

In this paper, the system (1) is assumed to be controllable and observable. To be more specific, the rank of the controllability matrix

$$\mathrm{rank}C_k = \mathrm{rank}[\mathbf{b} \ A\mathbf{b} \ A^2\mathbf{b} \ ... \ A^{n-1}\mathbf{b}] = n \quad (2)$$

and the rank of the observability matrix

$$\mathrm{rank}O = \mathrm{rank}\begin{bmatrix} C \\ CA \\ \vdots \\ CA^{n-1} \end{bmatrix} = n, \quad (3)$$

where n is the number of states of the system. When examining the SIMO-models, realization which is both controllable and observable is said to be minimal.

2.2 State feedback law

In this paper, state feedback control laws are written by [1]:

$$u(t) = K\mathbf{x}(t), \quad (4)$$

in which $u(t)$ and $\mathbf{x}(t)$ are respectively the same input and state vector as introduced in (1) and $K \in \mathbb{R}^{1 \times n}$ is called a full-state feedback gain. The control law in (4) assumes that the full state vector is known without any errors. If there are unknown states, it is mandatory to use a state estimator to calculate the missing values. When missing measurements represents rates of changes of state variables, then simple high-pass filters can be used to supplement the state such that state feedback control can be applied. In this paper, the high-pass filters are of the following form

$$\frac{\omega_f s}{s + \omega_f}, \quad (5)$$

where ω_f is the cut-off frequency of the filter and s is the Laplace variable. The filter (5) produces an estimate for the rate of change of its input signal.

The control law defined by the equation (4) is valid only with a regulation task. If the control scenario also includes a reference state vector $\mathbf{x}_r$, the closed-loop system consisting of (1) and (4) with the coordinate transformation $\tilde{\mathbf{x}} = \mathbf{x} - \mathbf{x}_r$ yields [1]:

$$\dot{\tilde{\mathbf{x}}} = \dot{\mathbf{x}} = (A - \mathbf{b}K)\tilde{\mathbf{x}} + A\mathbf{x}_r. \quad (6)$$

Therefore, there will always be steady-state error, unless $A\mathbf{x}_r = 0$. The condition $A\mathbf{x}_r = 0$ is met when the system matrix A is singular and the vector $\mathbf{x}_r$ belongs into the null space of this matrix, which is the situation in this paper.

2.3 Pole-placement method

Pole-placement is popular way to design control for closed-loop LTI-systems. Specifying desired locations of poles, a designer can ensure stability of the closed-loop and meet assigned control specifications. In theory, the closed-loop poles can be placed to arbitrary locations on the left-half complex plane if the system is controllable [2, 9]. Desirable places of the poles are achieved by choosing the correct coefficients to the gain matrix K.

There are a couple of different ways to calculate the correct value of the state gain matrix based on the given locations of poles. In this paper, feedback gain is calculated according to Ackermann's formula. The formula states that the state gain matrix K can be obtained by solving the equation [9, 10]

$$K = [0 \ 0 \ ... \ 0 \ 1]C_k^{-1}\alpha(A) \quad (7)$$

in which C_k is the controllability matrix from (2) and $\alpha(A)$ is defined by

$$\alpha(A) = A^n + \alpha_1 A^{n-1} + ... + \alpha_{n-1}A + \alpha_n I, \quad (8)$$

where $I^{(n \times n)}$ corresponds to $(n \times n)$ identity matrix and coefficients $\alpha_1, \alpha_2, ..., \alpha_n$ can be obtained from the desired characteristic polynomial

$$s^n + \alpha_1 s^{n-1} + ... + \alpha_{n-1}s + \alpha_n. \quad (9)$$

Ackermann's formula is feasible, because the system in this paper is well-conditioned and is of low-order.

2.4 Linear Quadratic Regulator

Linear quadratic regulator uses quadratic cost function to calculate the values of the state gain matrix K,

when the system is controllable [2]. In order to compare the results of optimizations, one has to declare a cost function J_k. An infinite horizon quadratic cost function, which is suitable for SIMO systems is

$$J_k = \int_0^\infty \mathbf{x}^\mathsf{T} Q \mathbf{x} + \mathrm{u}^2 R \; dt. \tag{10}$$

The vector $\mathbf{x}$ and the scalar u are from the state equation (1), whereas $Q \geq 0 \in \mathbb{R}^{n \times n}$ and $R > 0 \in \mathbb{R}$ are called weighting matrices [2].

An optimal state feedback gain, which minimizes the cost function (10) is [1]:

$$K = R^{-1} \mathbf{b}^\mathsf{T} P, \tag{11}$$

where $P > 0$ satisfies the algebraic Riccati equation [1]:

$$A^\mathsf{T} P + PA - P\mathbf{b}R^{-1}\mathbf{b}^\mathsf{T} P + Q = 0. \tag{12}$$

The Ricatti equation (12) is non-linear and can be solved e.g., using eigenvalues of the Hamiltonian matrix [1].

One can seek suitable weights by examining the physical characteristics of the system. Another approach for selecting the weights is trial and error, where initial selection (guess) is based on prior knowledge of the similar problems. The above-mentioned method of trial and error is often used at least in the final selection of weighting matrices. [1]

3 Transfer function matrix and Smith-McMillan form

A system's poles and, in the case of minimal realization of SIMO-system, transmission zeros can be found using Rosenbrock system matrix. Despite the usefulness of the Rosenbrock matrix, it could leave unrevealed information about the zeros of the system's transfer functions, which could cause nonminimal time domain behaviour. For this reason, a transfer function matrix is introduced. From the transfer function matrix, zeros and poles of the system is possible to determine using a system's Smith-McMillan form.

The transfer function matrix $G(s) \in \mathbb{C}^{l \times 1}$ of a SIMO-system is [11]

$$G(s) = C(sI - A)^{-1}\mathbf{b} \tag{13}$$

where matrices A, C and vector $\mathbf{b}$ are from equation (1). Poles and zeros of the transfer function from the input

u to l^{th} output can be found in the nominator and in the denominator of the corresponding element in G(s).

The theorem of the Smith-McMillan form states that a rational matrix G(s) of normal rank n could be transformed into a pseudo-diagonal rational matrix [12]

$$\mathrm{M(s)} = diag\left\{\frac{\varepsilon_1(s)}{\psi_1(s)}, \frac{\varepsilon_2(s)}{\psi_2(s)} ... \frac{\varepsilon_r(s)}{\psi_r(s)}, 0, ...0\right\} \tag{14}$$

in which polynomials $\frac{\varepsilon_i(s)}{\psi_i(s)}$ $(i = 1, 2, ..., r - 1)$ have no common factors and

$$\begin{cases} \varepsilon_i(s)/\varepsilon_{i+1}(s) \\ \psi_{i+1}(s)/\psi_i(s) \end{cases} \tag{15}$$

are satisfied without remainder. The diagonal matrix M(s) is called the Smith-McMillan form of the transfer function matrix G(s), and in the case of SIMO-system, it reduces to

$$\mathrm{M(s)} = diag\left\{\frac{\varepsilon_1(s)}{\psi_1(s)}\right\} = \begin{bmatrix} \frac{\varepsilon_1(s)}{\psi_1(s)} \\ 0 \end{bmatrix}. \tag{16}$$

3.1 System's poles and zeros from the Smith-McMillan form

Poles of the system can be found from the roots of the pole polynomial of the constructed Smith-McMillan form. The pole polynomial is defined by denominators of M(s) as [12]

$$p(s) = \psi_1(s)...\psi_r(s), \tag{17}$$

which in SIMO-case only contains the first element $\psi_1(s)$. If the realization is minimal, the pole polynomial is given by $\det(sI - A)$ and the poles are the eigenvalues of the system matrix A.

In general, when the system is not in the form of SISO, there is defined different kind of zeros, called invariant zeros. In the case of minimal realization, the invariant zeros are the same as transmission zeros. Transmission zeros are found from the roots of the zero polynomial of Smith-McMillan form, where zero polynomial is [12]

$$z(s) = \varepsilon_1(s)...\varepsilon_r(s). \tag{18}$$

In SIMO-case, the zero polynomial is reduced to contain only the numerator $\varepsilon_1(s)$ of the fist element of M(s).

4 Quanser QUBE-Servo 2 system

Quanser QUBE-Servo 2 system is a rotary DC motor application, which can be used as a testbed for

reference tracking and regulation tasks. It consist of an Allied Motion CL40 Series 18V brushed DC motor (model 16705) and a PWM (Pulse-Width Modulation) voltage-controlled power amplifier, which is used to power the motor. The PWM accepts commands from Data Acquisition (DAQ) device. The DAQ is linked to a PC via USB connection. Quanser also provides Simulink/Matlab add on (QUARC), which includes necessary blocks to use the unit with Simulink software.

The rotary inverted pendulum is attached to the DC motor via magnets. Angular positions of the DC motor and the pendulum are measured with a single-ended optical shaft encoder (US Digital E8P-512-118) with the resolution of 2048 counts per revolution, which transforms to 0.176 degree of accuracy. The sampling rate of the angle measurements is 0.001 second. Rotary pendulum attached to Quanser QUBE-Servo 2 is depicted in Fig. 1. A more detailed description of the specifications of the unit can be found from the datasheet of the manufacturer.

Fig. 1. Quanser QUBE-Servo 2 system with the rotary pendulum

The equations of motion (EOM) of the rotary pendulum system is obtained using Euler-Lagrange method and defined by two non-linear differential equations:

$$(m_p L_r^2 + \frac{1}{4} m_p L_p^2 - \frac{1}{4} m_p L_p^2 cos(\alpha)^2 + J_r)\ddot{\theta}$$
$$- (\frac{1}{2} m_p L_p L_r cos(\alpha))\ddot{\alpha} + (\frac{1}{2} m_p L_p^2 sin(\alpha)cos(\alpha))\dot{\theta}\dot{\alpha}$$
$$+ (\frac{1}{2} m_p L_p L_r sin(\alpha))\alpha^2 = \tau - D_r\dot{\theta} \tag{19}$$

$$\frac{1}{2}m_p L_p L_r cos(\alpha)\ddot{\theta} + (J_p + \frac{1}{4}m_p L_p^2)\ddot{\alpha}$$
$$- \frac{1}{4}m_p L_p^2 cos(\alpha)sin(\alpha)\dot{\theta}^2$$
$$+ \frac{1}{2}m_p L_p g sin(\alpha) = -D_p\dot{\alpha}, \tag{20}$$

and

$$\tau = \frac{k_m(V_m - k_m\dot{\theta})}{R_m}, \tag{21}$$

where θ is a rotary arm angle, $\dot{\theta}$ is the angular speed of the rotary arm angle, $\ddot{\theta}$ is the angular acceleration of the rotary arm, α is the inverted pendulum angle, $\dot{\alpha}$ is the angular velocity of the inverted pendulum angle and $\ddot{\alpha}$ is angular acceleration. The input voltage to the system is V_m. The remaining constants are the arms mass (m_r, m_p), the arms length (L_r, L_p), the equivalent viscous damping coefficients (D_r, D_p), the moments of inertia about pivot (J_r, J_p), the terminal resistance of the DC motor R_m, torque constant k_t and back-emf constant k_m. The subscripts 'r' and 'p' refer to the rotary arm and the inverted pendulum, respectively. The value of the inverted pendulum angle is zero when the pendulum is in the downward position. Numerical values of the parameters are listed in Table 1.

Table 1. Quanser QUBE-Servo 2 parameters

Symbol	Description	Value
	Rotary arm	
m_r	Rotary arm mass	0.095 kg
L_r	Rotary arm length	0.085 m
D_r	Equivalent Viscous Damping Coefficient	0.0015 $\frac{\text{Nms}}{\text{rad}}$
J_r	Moment of inertia about the center of mass	5.7 ×10^{-5} kgm^2
	Pendulum link	
m_p	Pendulum link mass	0.024 kg
L_p	Pendulum link lenght	0.13 m
D_p	Equivalent Viscous Damping Coefficient	0.0005 $\frac{\text{Nms}}{\text{rad}}$
J_p	Moment of inertia about the center of mass	3.4 ×10^{-5} kgm^2
	DC Motor	
R_m	Terminal resistance	8.4 Ω
k_t	Torque constant	0.042 $\frac{\text{Nm}}{\text{A}}$
k_m	Back-emf constant	0.042 $\frac{\text{Vs}}{\text{rad}}$

The moments of inertia J_p and J_r in Table 1 are calculated by

$$J_p = \frac{1}{12}m_p L_p^2 \quad \text{and} \quad J_r = \frac{1}{12}m_r L_r^2. \tag{22}$$

The kinematics of the inverted pendulum system is sketched in Fig. 2. In Fig. 2, Cartesian axes are labeled

as x_0, y_0 and z_0, θ is the rotary arm angle, α is the pendulum link angle, L_r is the rotary arm length and L_p is the pendulum link length.
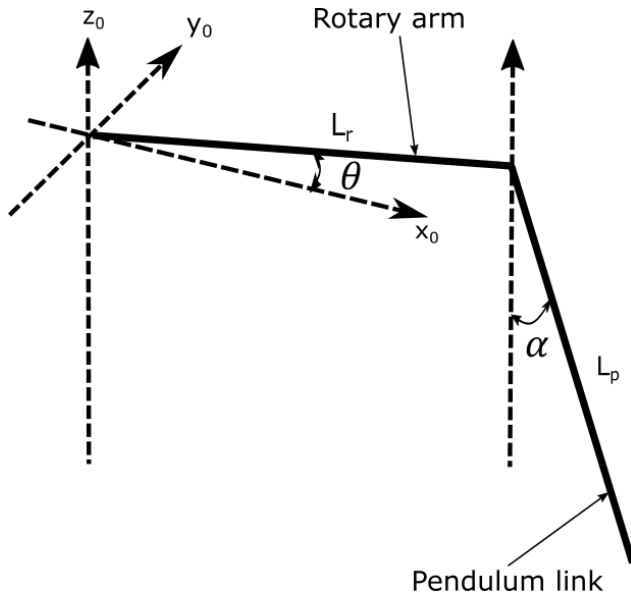

Fig. 2. Kinematics of the inverted pendulum

Equations (19) and (20) must be linearized for LTI-control algorithms introduced previously in this paper. Linearization is performed at the point where the pendulum link angle $\alpha = 180° = \pi$ rad, and the rotary arm angle $\theta = 0°$. The linearized EOM are

$$\begin{cases} (m_p L_r^2 + J_r)\ddot{\theta} + (\frac{1}{2}m_p L_p L_r)\ddot{\alpha} & = \tau - D_r\dot{\theta} \\ (-\frac{1}{2}m_p L_p L_r)\ddot{\theta} + (J_p + \frac{1}{4}m_p L_p^2)\ddot{\alpha} & \\ +(-\frac{1}{2}m_p L_p g)\alpha & = -D_p\dot{\alpha}. \end{cases} \quad (23)$$

Using the values from Table 1 and substituting equation (21) to equation (23), the state-space model of the QUBE-Servo 2 system can be written as

$$\begin{bmatrix} \dot{\theta} \\ \dot{\alpha} \\ \ddot{\theta} \\ \ddot{\alpha} \end{bmatrix} = \begin{bmatrix} 0 & 0 & 1 & 0 \\ 0 & 0 & 0 & 1 \\ 0 & -41.6 & -4.16 & 1.37 \\ 0 & 72.4 & -4.11 & -2.40 \end{bmatrix} \begin{bmatrix} \theta \\ \alpha \\ \dot{\theta} \\ \dot{\alpha} \end{bmatrix} + \begin{bmatrix} 0 \\ 0 \\ 13.9 \\ 13.7 \end{bmatrix} V_m$$

$$\begin{bmatrix} \theta \\ \alpha \end{bmatrix} = \begin{bmatrix} 1 & 0 & 0 & 0 \\ 0 & 1 & 0 & 0 \end{bmatrix} \begin{bmatrix} \theta \\ \alpha \\ \dot{\theta} \\ \dot{\alpha}. \end{bmatrix}$$

and $\mathbf{x}_0 = \begin{bmatrix} 0 & 0 & 0 & 0 \end{bmatrix}^\mathsf{T}$. The controllability and observability matrices are both full rank, and hence, the state-space model (24) is the minimal realization of the inverted pendulum system. Thus, the invariant zeros

are equivalent to the transmission zeros. The transfer function matrix of the QUBE-Servo 2 system from the state-space model (24) is represented as

$$G(s) = \begin{bmatrix} \frac{13.9s^2+52.1s-1582}{s^4+7.14s^3-55.1s^2-541s} \\ \frac{13.7s-1.79\times10^{-6}}{s^3+7.14s^2-55.1s-541} \end{bmatrix}. \quad (25)$$

Using the algorithm in [12], the Smith-McMillan form of the system is:

$$M(s) = \begin{bmatrix} \frac{1}{s^4+7.14s^3-55.13s^3-541s} \\ 0 \end{bmatrix}, \quad (26)$$

in which the zero polynomial $z(s) = 1$ and the pole polynomial $p(s) = s^4 + 7.14s^3 - 55.1s^2 - 541s$. The above indicates that the rotary pendulum does not have any transmission zeros and the pole locations on the complex plain are $s = 0$, $s = 8.05$ and $s = -7.60 \pm 3.08i$, so the pendulum must be stabilized using feedback control.

5 Feedback controllers

In this paper, the designed controllers must satisfy three requirements:
- The control input V_m has to be between $\pm 15V$.
- The deviation of the pendulum link angle α must be kept with ± 20 degrees from the upright position.
- The rotary arm and pendulum should be moved from the given initial position to final position swiftly without causing overshoot or oscillation.

The first restriction is due to limited performance of the DC motor. The second is involved because of so-called swing-up control that Quanser has implemented for raising the pendulum link to the upright position.

As mentioned in Section 1, the performances of the closed-loop systems are evaluated using rise time (t_r), settling time (t_s) and maximum overshoot (M_p) of the response of the rotary arm. The rise time is defined to be the time in which the response rises from 10% to 90% of its final value. The settling time is the time which the system's response takes to settle 2% from its steady-state value, and the maximum overshoot is the percentage of the maximum value of the response compared to its final value.

Measurements from both angles θ and α are directly provided by QUBE-Servo 2 hardware, whereas the rate of changes of the θ and α are provided by the following high-pass filters

$$\frac{50s}{s+50}. \quad (27)$$

The filters transfer function (27) is provided by Quanser.

First, pole-placement method is used to compose the full-state gain matrix K. The locations of selected poles are

$$s = -5, \quad s = -8.8 \pm 5i \quad \text{and} \quad s = -10. \tag{28}$$

The characteristic polynomial (9) constituted from poles (28) is

$$s^4 + 32.6s^3 + 416.4s^2 + 2416.6s + 5122. \tag{29}$$

Using the system's controllability matrix and the coefficients of the characteristic polynomial (29), Ackermann's formula (7) yields

$$K = \begin{bmatrix} -3.2488 & 45.2021 & -1.9767 & 3.8578 \end{bmatrix}. \tag{30}$$

Competing LQR-design is achieved by selecting the weighting matrices for the cost function (10), and minimizing it by solving the algebraic Ricatti equation (12). After comparing the formed possible gain matrices, the one designed with LQR method performed in the best way i.e. the response yielded the smallest numbers for the chosen performance indicators. The chosen weights were

$$Q = \begin{bmatrix} 15 & 0 & 0 & 0 \\ 0 & 4 & 0 & 0 \\ 0 & 0 & 0.5 & 0 \\ 0 & 0 & 0 & 0.2 \end{bmatrix} \quad \text{and} \quad R = 1. \tag{31}$$

The weights in (31) results in the state feedback gain given by

$$K = \begin{bmatrix} -3.8730 & 51.2299 & -2.2650 & 4.3458 \end{bmatrix}. \tag{32}$$

The optimal state gain matrix (32) assigns the system's poles to the locations $s = -5.10, s = -9.88 \pm 4.19i$ and -10.4.

5.1 Simulation results

The simulation model is constructed using the linearized state-space representation (24). Connecting the state gain matrix (32) with the filters (27) to control the inverted pendulum yields the step responses of the pendulum link angle α and the rotary arm angle θ, which are represented in Fig. 3. Corresponding values of the input voltage V_m is in Fig. 4. The size of the step of the rotary arm angle in reference state $\mathbf{x}_r$ is $\frac{\pi}{2}$ rad (90 degrees). There are also Gaussian measurement noise included with mean = 0, variance = 1, sample time = 0.01, and which is multiplied by 0.001.
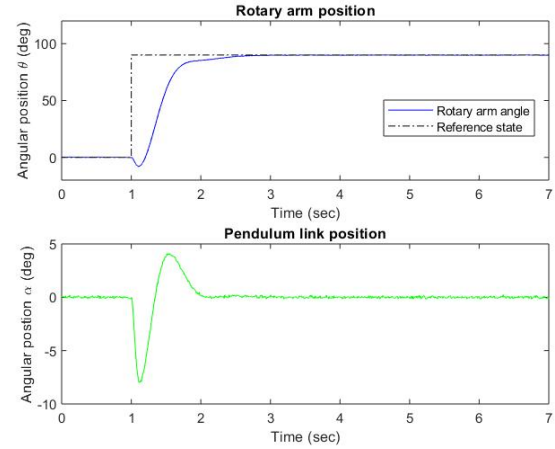

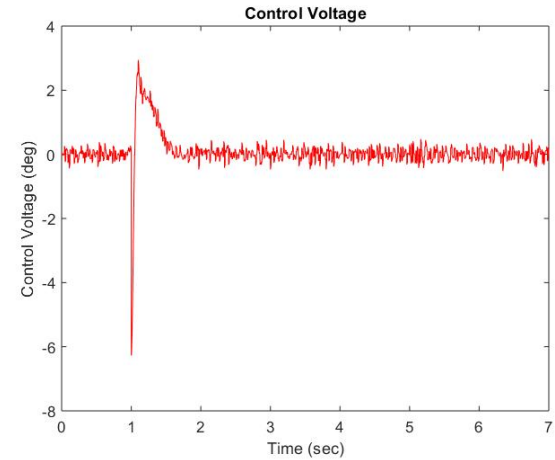**Fig. 3.** Reference tracking of the simulated closed-loop system

Fig. 4. Control voltage of the simulated LQR controller

According to Fig. 3 and Fig. 4, the control requirements are satisfied. The step response of the rotary arm angle has no overshoot and the settling time is 1.37 seconds. The input voltage (±6.5 V) is well below the given limits, and the maximum deviation of the pendulum angle is approximately 8 degree from the upright position. Therefore, it is possible to use even larger step change of the reference state. As expected from (6), the state error is driven to zero, because $A\mathbf{x_r} = 0$.

The influence of the zeros of the inverted pendulum can be seen from the angle responses. To analyze the effect of zeros, we look back at the system (25). Both transfer function elements in the matrix have nonminimal zero(s), which causes the inverted behavior at the beginning of the step responses. When the DC motor starts turning, the upright positioned pendulum link deviates to the wrong direction due to the moving

rotary arm and the gravitation. To be able to track the given reference state, without tipping over the link, DC motor has to perform the corrective move to be able to maintain its balancing property.

5.2 Implementation results

The Simulink model of the physical QUBE-Servo 2 unit differs from that of the one used in Section 5.1 and is found from the documentation of the pendulum link system by Quanser. Difference between the model used in this paper and the one by Quanser is caused by compensation term due to relative measurement of the angles. In practice, the compensation term causes the activation of the step signal to take place at the same moment as the reference state changes. That produces an offset to the response of the rotary arm angle before the step change. With the compensation term, responses of the angles θ and α are in Fig. 5 and values of the input voltage in Fig. 6. The step change of the reference state of the rotary arm angle is the same magnitude $\left(\frac{\pi}{2}\right)$ as in the simulations. The zero value of the pendulum link angle is defined to be in the lower position, so values of the y-axis in Fig. 5 are +180 degrees compared to simulation results.
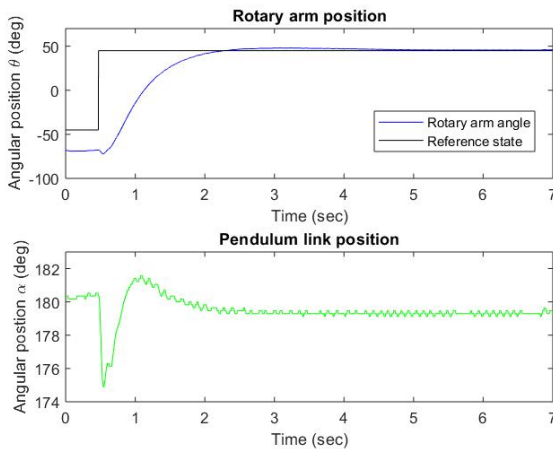

Fig. 5. Experimental result of the angular position of closed-loop system

The performance of the system is similar compared to simulation results in Section 5.1. Both of the given restriction is met with secure margins, and there is practically no steady-state error as discussed in Subsection 2.2. The model of the system does not describe the pendulum system accurately, so the
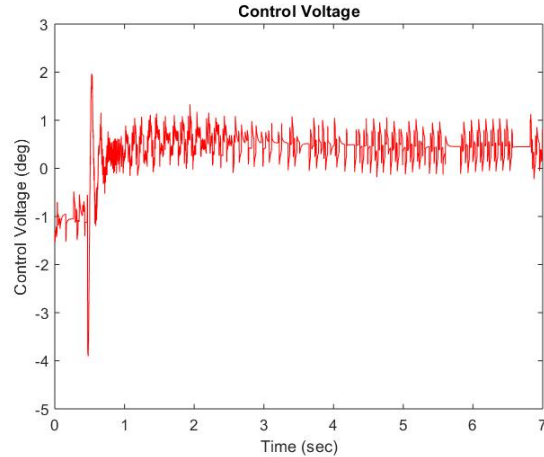

Fig. 6. Experimental result of the control voltage of chosen LQR controller

experimental response of the rotary arm poses a slight overshoot. The resolution of the pendulum link measurement is seen from the constant vibration of the pendulum link position. The vibration is also due to balancing movements of the DC motor, which stabilize the pendulum link to the upright position. The transient response characteristics of the system are

$$M_p = 2.48 \quad t_s = 3.90 \quad \text{and} \quad t_r = 0.966. \qquad (33)$$

The performance could slightly be improved with a parallel-connected integrating controller. The disadvantage of that approach is the selection of the integration gain which could lead, in the worst scenario, to more oscillating responses and even instability of the system. The effect of the minimal-zeros of the system is in line with the simulation result. As mentioned in Section 5, the stability of the system is sensitive to small changes in the values in state gain matrix.

6 Conclusion

In this paper, we have designed an LQR state feedback controller for Quanser QUBE-Servo 2 inverted pendulum system. The LQR controller was not only able to stabilize the system, but it also satisfied all control requirements and design constraints. The closed-loop system yielded fast and accurate set-point tracking of the rotary arm angle despite of nonminimum phase system characteristics. The controllers presented in this paper could also be potentially used in other applications e.g., in Segway kind of conveyors.

References

[1] Burl J. B., Linear Optimal Control, H_2 and H_{inf} Methods, Addison Wesley Longman Inc., Menlo Park, Calif., 1999

[2] Belanger P. R., Control Engineering: A Modern Approach, Saunders College Publ., Fort Worth : New York (NY), 1995

[3] Muskinja N., Tovornik B. A., Swinging up and stabilization of a real inverted pendulum, IEEE Transactions on Industrial Electronics, 2006, 53, 631-639, DOI: 10.1109/TIE.2006.870667

[4] Pathak K., Franch K., Agrawal S. K., Velocity and position control of a wheeled inverted pendulum by partial feedback linearization, IEEE Transactions on Robotics, 2005, 21, 505-513, DOI: 10.1109/TRO.2004.840905

[5] Hehn M., D'Andrea R., A flying inverted pendulum, 2011 IEEE International Conference on Robotics and Automation (9 May - 13 May 2011, Shanghai, China), IEEE, Shanghai, 2011, 763-770

[6] Matsuoka K., Williams V., Learning to balance the inverted pendulum using neural networks, Proceedings of the 1991 IEEE International Joint Conference on Neural Networks (18 November - 21 November 1991, Singapore, Singapore), IEEE, Singapore, 1991, 214-219

[7] Takei T., Imamura R., Yuta S., Baggage Transportation and Navigation by a Wheeled Inverted Pendulum Mobile Robot, IEEE Transactions on Industrial Electronics, 2009, 56, 3985-3994, DOI: 10.1109/TIE.2009.2027252

[8] Tang Z., Joo Er M., Humanoid 3D Gait Generation Based on Inverted Pendulum Model, 2007 IEEE 22nd International Symposium on Intelligent Control (1 October - 3 October 2007, Singapore, Singapore), IEEE, Singapore, 2007, 339–344

[9] Williams II R. L., Lawrence D. A., Linear State-Space Control Systems, John Wiley & Sons, Inc., Hoboken, New Jersey, 2007

[10] Ogata K., Modern Control Engineering, 5th ed., Pearson Education Inc., Prentice Hall, 2010

[11] Glyn J., Advanced Modern Engineering Mathematics, 3rd ed., Pearson Education Limited, Harlow, 2011

[12] Maciejowski J.M., Multivariable feedback design, Addison-Wesley Publishers Ltd., Wokingham, 1989